Surface Nanocrystallization of 310S Stainless Steel and Its Effect on Oxidation Behavior

Z. Liu, Y. He, and W. Gao

(Submitted 14 April 1997; in revised form 1 September 1997)

Two techniques, unbalanced magnetron sputter deposition and high-energy short-pulsed plasma discharge, have been used to produce a nanocrystalline surface on AISI 310S stainless steel specimens. The average grain size after surface modification was estimated as ~100 nm by using atomic force microscopy. Cyclic oxidation was performed at 1000 °C with treated and untreated 310S stainless steel specimens. The oxide products formed on the specimens consisted of an outer spinel layer that was rich in chromium, iron, manganese, and nickel, and an inner chromium-rich layer. It was found that the concentrations of iron and manganese in the outer layer of treated specimens were higher, and adherence of the scale was better in the treated specimens. The observed oxidation behavior can be explained by the increase of the creep diffusion rate in the fine oxide scale formed on the nanocrystalline surfaces.

Keywords 310S steel, magnetron sputtering, nanocrystallization, oxidation

1. Introduction

AISI 310S stainless steel is an important commercial alloy that is widely used in applications associated with high temperatures. Its high-temperature oxidation resistance is one of the most important properties. Previous research (Ref 1), however, showed in some environments that the oxide spallation resistance at 1000 °C was not satisfactory, although the alloy contains a high chromium content (~25 wt% Cr).

A number of researchers have reported that surface microcrystallization is an effective way to improve the oxidation resistance of alloys (Ref 2, 3). It is believed that the beneficial effects of surface microcrystallization on the oxidation behavior of stainless steels can be attributed to: (a) the enhancement of chromium diffusion to the surface along grain boundaries, (b) the release of the stresses stored in the oxides, and (c) the mechanical "keying" effects of oxides to the high concentration of grain boundaries of the substrate metal.

A variety of techniques have been developed to produce surface micro- and nanocrystallization. Among them, unbalanced magnetron sputter deposition (UMSD) is a popular method. The UMSD method and a newly developed method, high-energy short-pulsed plasma discharge (HESPPD), were used to produce nanocrystalline surfaces on 310S stainless steel specimens. The average grain size in the treated surface layers was less than 100 nm. Cyclic oxidation testing was conducted with the treated and untreated specimens at 1000 °C. Both the oxidation and spallation kinetics were measured. In order to study the effects of nanocrystallization on the oxidation behaviors, the samples did not undergo separate vacuum annealing before oxidation testing.

Z. Liu, Y. He, and **W. Gao,** Department of Chemical and Materials Engineering, The University of Auckland, Private Bag 92019, New Zealand.

2. Experimental Procedure

The chemical composition of the stainless steel used in this work is shown in Table 1. Specimens were prepared to the dimensions of 3.0 by 10.0 by 15.0 mm.

In the UMSD method, a single target of 310S stainless steel was used. The predeposition procedure consisted of 90 min of radio frequency (RF) plasma substrate cleaning and 5 min of target cleaning. The deposition time was 120 min. The argon pressure during deposition was 0.066 Pa (0.5 mTorr). The distance between the substrate and target was ~125 mm. During deposition, substrates were rotated in front of the target at a rate of 4.2 rpm.

The HESPPD method has been developed for surface treatment. Figure 1 shows a schematic drawing of the technique. The treated specimen was used as one electrode, and a pure aluminum was used as another electrode. The discharging pulse width was ~60 μs with the voltage of ~10,000 V, the discharging interval time was ~3 s, and the distance between the two discharging points was 1 mm. When electrons were discharged between the specimen and the aluminum rod, extremely high

Table 1 Chemical composition of 310S stainless steel (wt%)

C	Si	Mn	P	S	Ni	Cr	Fe
0.04	0.61	0.97	0.016	0.001	19.50	25.0	bal

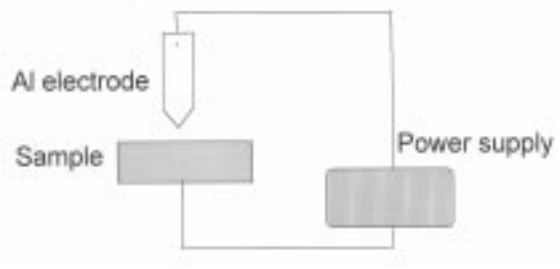

Fig. 1 A schematic drawing of the HESPPD technique

energy was released as a spark in a very short period of time. The local temperature can be raised to ~20,000 °C. The high energy means that the surface can be melted and resolidified within a very short time. The surface micro- or nanocrystalline structures were formed due to the extremely high cooling and solidification rates.

Oxidation testing was performed in a horizontal furnace at 1000 °C for up to 200 h in ambient atmosphere. Temperature accuracy in the hot zone of the furnace was within ±1 K. Each specimen was held in a quartz crucible so that the spalled oxides could be collected and measured. After the required period of time, the crucibles were removed from the furnace and cooled to room temperature. The total weight change of a specimen plus crucible and the net weight change of the specimen were measured and recorded. The specimens were then placed back in the hot zone of the furnace for the next thermal cycle.

An atomic force microscope (AFM) was used to observe the morphologies of the specimens before and after treatments. Scanning electron microscopy (SEM) was used to study the cross sections of oxide scales. Energy dispersive spectroscopy (EDS) was used to determine the chemical compositions of the oxide scales. X-ray diffraction (XRD) with Co-K_α radiation was used to study the changes in crystal structures before and after treatments, and in the oxide scales.

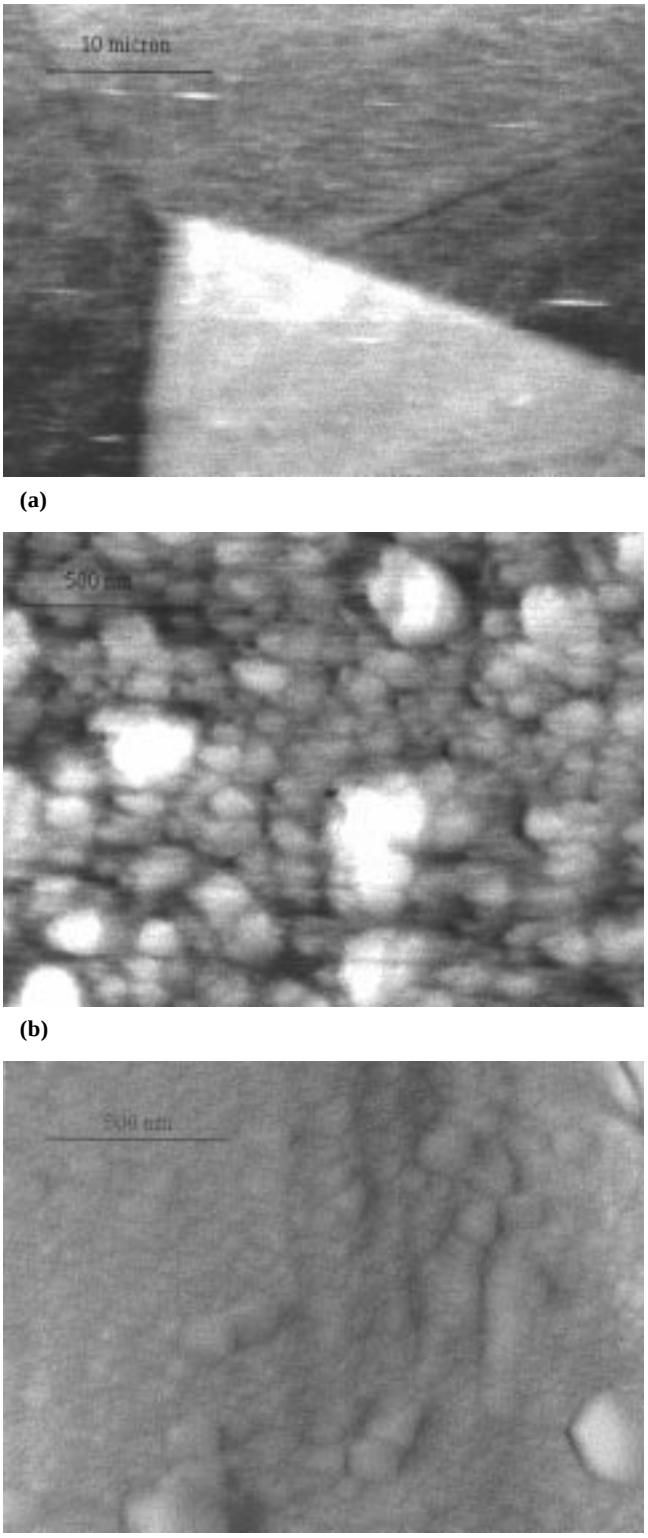

(a)

(b)

(c)

Fig. 2 AFM images of the (a) untreated, (b) UMSD, and (c) HESPPD 310S stainless steel samples

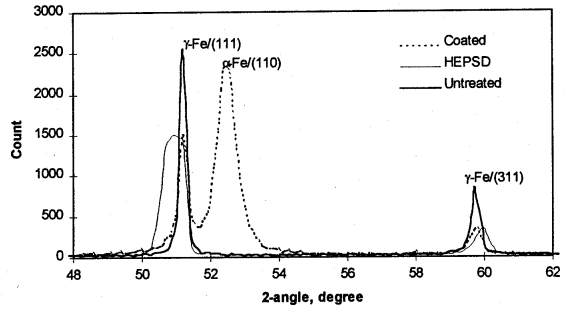

Fig. 3 The XRD spectrum of the treated and untreated specimens

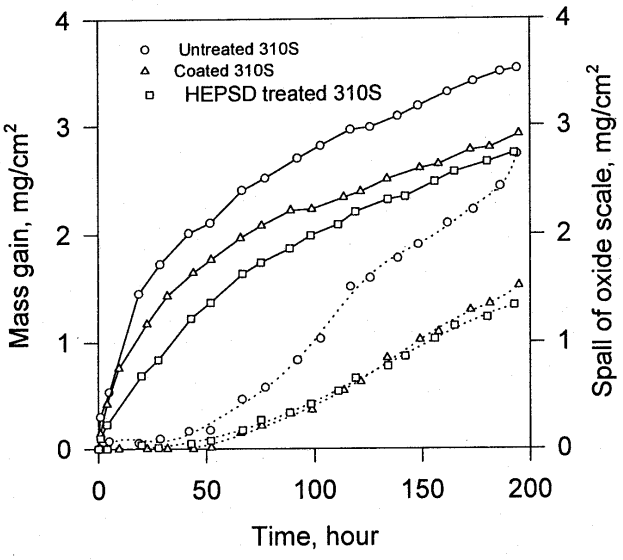

Fig. 4 The oxidation and spallation kinetics of UMSD, HESPPD, and untreated 310S specimens (at 1000 °C)

3. Results and Discussion

Figures 2(a) to (c) show the AFM morphologies of the 310S stainless steel samples. Figure 2(a) shows the surface morphology of an untreated 310S specimen, which was etched before AFM observation. The grain size of the untreated steel was estimated as ~100 μm. Figures 2(b) and (c) show the surface morphologies of the UMSD and HESPPD specimens, respectively. The average grain sizes were ~100 nm and <100 nm for the UMSD and HESPPD surfaces, respectively. The surface treated by using HESPPD is flatter than the surface treated by UMSD.

Figure 3 shows the XRD patterns of the treated and untreated specimens. For the untreated and HESPPD specimens, the XRD patterns show only austenite peaks. The XRD of the UMSD coating shows a strong ferrite/(110) peak and a few weak austenite peaks. The weak austenite peaks are believed to be from the 310S stainless steel substrate (austenitic steel). While UMSD produces a coating with ferritic structures, the structure of the steel treated with HESPPD remains austenitic. Furthermore, the XRD patterns of the HESPPD and UMSD specimens show much wider peaks than the patterns of the untreated 310S specimens, indicating the formation of micro- and nanocrystalline structures, and/or stress generation on the surface layer due to the treatment.

Figure 4 shows the oxidation and spallation kinetics of the UMSD, HESPPD, and untreated specimens during oxidation testing at 1000 °C. The HESPPD specimen shows the lowest total mass gain and a spallation behavior similar to that of the UMSD specimen. Compared to the untreated specimen after ~200 h of oxidation, the total mass gain for the two treated specimens was decreased by ~30%, and the total spallation weight of the treated specimens was decreased by ~100%, indicating that the treated specimens possessed lower oxidation rates and much better spallation resistance than the untreated specimen. After 50 h of oxidation, the spallation weights of the UMSD and HESPPD specimens were 0.2 and 0.5 g/m^2, respectively, while the spallation weight of the untreated specimen after 5 h of oxidation was 0.75 g/m^2, showing that spallation took place on the untreated specimen much earlier than on the treated ones.

XRD was used to identify the phase structures of the oxidation products. Chromia and a spinel phase were found in the spectra. Due to the relatively high chromium content (25 wt%), chromia was easily formed on the untreated and treated specimens. This explains why the difference in total mass gain was not large.

Figure 5 shows the SEM micrographs of cross sections of the oxide layers. Elemental distributions are shown beside the SEM images. It can be seen that the outer layer spinel is rich in iron, manganese, chromium, and nickel, and that the inner layer is slightly richer in nickel than the substrate metal. In the base metal, there is a chromium depletion zone. Silicon-selective oxidation was found to take place in the grain boundary areas beneath the oxide scale. In the outer spinel layer, the chromium concentrations of the surface-treated specimens were lower, and the iron and manganese concentrations were higher than in the untreated specimens. This implies that the flux of iron and manganese from the alloy to the outer layer oxide was accelerated during oxidation by microcrystallization treatment.

Generally speaking, an increase of iron and manganese concentrations in the oxide scales is not beneficial to the oxidation resistance of the alloy. However, from the experimental results, it can be seen that the spallation resistance of the treated specimens was obviously improved. This improvement may have resulted from two factors: (a) the adherence between the oxide scale and base metal was improved, and (b) the stresses between the oxide and base metal were easily released due to the surface microcrystallization treatment.

The stresses in the oxide scales or between the oxide and metal generally consist of growth stress and thermal stress (Ref 4, 5). The growth stress accumulates during the oxidation process, while the thermal stress is mainly produced by cooling and heating the specimens. The accumulation of stresses may result in cracking and detachment of the oxide scales. However, these stresses can be released at elevated temperature due to the diffusion creep. The diffusion creep rate, $\dot{\varepsilon}$, is expressed as (Ref 6-8):

$$\dot{\varepsilon} = \frac{\Omega\sigma}{d^2 kT}\left(B_1 D_L + \frac{B_2 D_B \delta}{d}\right) \quad \text{(Eq 1)}$$

where d is the average grain size, δ is the grain boundary thickness, k is Boltzmann's constant, σ is the tension stress, B_1 and B_2 are constants, Ω is the atomic volume, and D_B and D_L are the diffusion coefficients through grain boundaries and the lattice, respectively.

Equation 1 indicates that if the oxide grain size is reduced by one order of magnitude, the diffusion creep strain rate can be increased by approximately 2 to 3 orders of magnitude. The oxide grains formed on a micro- or nanocrystalline alloy, especially at the early stage of oxidation, are much smaller than those formed on an alloy with normal grain size, because there are many more nucleation sites on the microcrystalline alloy than on an ordinary alloy. The stresses stored in the oxide scales, therefore, can be released more effectively in a microcrystalline alloy. The accumulation rate of the fracture energy then can be reduced. This means that the adhesion between the oxide scale and base metal is improved due to the alloy microcrystallization. With the oxidation reaction going on at high temperatures, the diffusion creep rate decreases because of the oxide grain growth. As a result, the grain size effect is less significant, and all of the specimens show a similar spallation tendency after long-time oxidation.

4. Conclusions

Micro- or nanocrystalline layers were obtained by using UMSD and HESPPD on the surface of 310S stainless steel samples. The average grain sizes were ≤100 nm. After oxidation testing, the scale spallation resistance of the specimens with surface microcrystallization treatment was improved by ~100%, compared to that of the untreated specimens. The improvement in spallation resistance can be explained by the stress release due to creep diffusion in the fine oxide grains that were formed on the micro- or nanocrystallized surfaces.

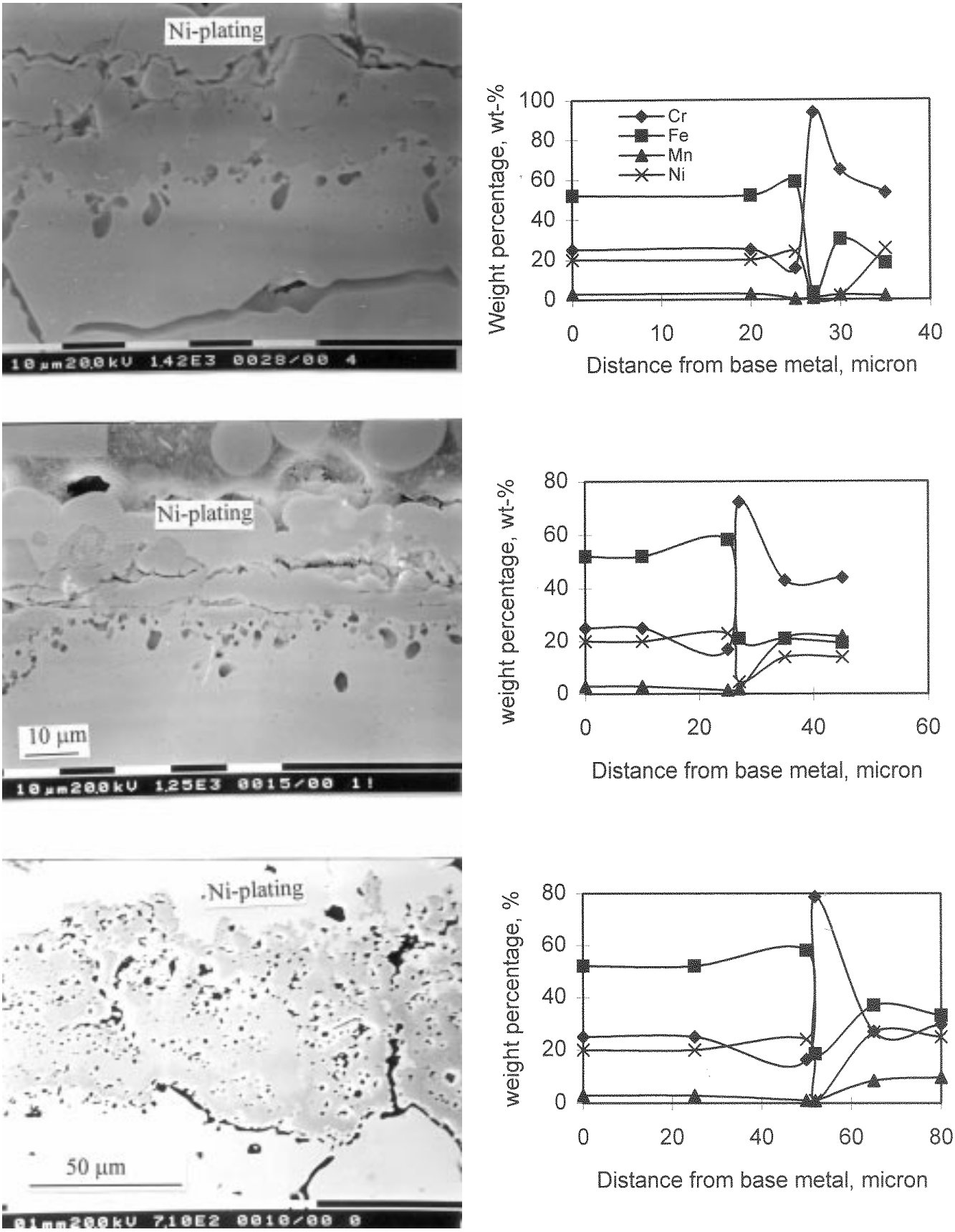

Fig. 5 SEM micrographs of cross sections of (a) untreated, (b) UMSD, and (c) HESPPD specimens

Acknowledgments

This project was supported by a FRST Grant UOA505. The authors would like to thank Dr. G.A. Wright, Mr. K. Dahm, Miss M. Prasad, and the technical staff in the Department of Chemical and Materials Engineering and the Centre for Surface and Materials Research.

References

1. F.H. Stott and F.I. Wei, *Mater. Sci. Technol.*, Vol 5, 1989, p 1140-1147
2. M.D. Merz, *Metall. Trans.*, Vol 10A, 1979, p 71-77
3. H. Lou, F. Wang, S. Zhu, B. Xia, and L. Zhang, *Surf. Coat. Technol.*, Vol 63, 1994, p 105-114
4. R.C. Lobb and H.E. Evans, *Met. Sci.*, June 1981, p 267-274
5. S.N. Basu and G.J. Yurek, *Oxid. Met.*, Vol 36, 1991, p 281-315
6. P. Kofstad, *High Temperature Corrosion*, Elsevier Applied Science Publisher Ltd., London, 1988
7. Y. He, Z. Liu, and W. Gao, The Influence of Surface Nano-Crystallisation on the Cyclic Oxidation of 304 Stainless Steel, paper presented at the Institution of Professional Engineers of New Zealand Conference, 1997, New Zealand
8. J. Karch, R. Birringer, and H. Gliaiter, *Nature*, Vol 330, 1987, p 556